Electroless Addition of Platinum to SnO_2 Nanopowders

Raül Díaz,*,† Jordi Arbiol,‡ Fausto Sanz,† Albert Cornet,‡ and Joan R. Morante‡

Department of Physical Chemistry and Enginyeria i Materials Electrònics, Department of Electronics, University of Barcelona, Martí i Franqués, 1, Barcelona 08028, Spain

Received October 11, 2001. Revised Manuscript Received May 14, 2002

A procedure based on electroless metal deposition using Sn(II) as the reductor, previously used for the efficient addition of controlled amounts of Pd to nanoscaled SnO_2 powders, is now applied to add Pt, which is also an important sensitizer of semiconductor gas sensors. This study was performed with the aim of studying the possible application of this method for the addition of other metals, regardless of the appearance of new chemical features. The characterization of these powders using XRD, Raman spectroscopy, XPS, ICP, and HRTEM is presented and discussed, showing the feasibility of the proposed catalyst addition mechanism as a useful tool for improving of existing catalytic materials for gas sensors, even using different chemical reagents because of chemical restrictions, as happens in the case of platinum. A set of platinum salt concentrations and reducing agent ratios, as well as different annealing temperatures, was used to analyze the influence of these parameters on the morphology and composition of the samples. The results indicated the presence of homogeneously distributed metallic Pt nanoclusters of only a few nanometers in size on the SnO_2 nanopowder surface.

Introduction

After Brattain and Bardeen demonstrated, as early as in 1953, that gas adsorption at the surface of Ge leads to a significant variation of the conductance,[1] the first structures to be used as chemical gas sensors, making use of this phenomenon, were attributed to Seiyama[2] and Taguchi[3] in 1962. Since then, sensing materials exhibiting changes in conductivity upon gas exposure have become a topic of wide study, tin(IV) oxide (SnO_2) being the most used material mainly because of its high reactivity to reducing gases at relatively low temperatures.[4,5] Currently, research is mainly directed toward increasing the capabilities of existing sensors, so that the main restrictions that these sensors present—low sensitivity, low selectivity, and low stability—can be overcome. Thus, it has been demonstrated that the use of sensing material on the nanoparticle scale improves the response (sensitivity) of the chemical sensor,[6,7] and the introduction of small quantities of noble metals, such as platinum, catalyzes the sensitivity to a certain gas (i.e., improves selectivity) and lowers sensing temperatures (i.e., improves stability).[8−10] Both sensitivity and selectivity also depend on the distribution, chemical state,[11] and crystal size of the added noble metals[8,12] and, consequently, on the procedure used to obtain the sensing material. Impregnation has been the most frequently used addition method[4,8,11,13] because of its simplicity and low cost.

In this context, the aim of this paper is to study the feasibility of a recently developed addition process that we have performed for Pd[14] as a general method for depositing metals on SnO_2. The advantages of the proposed technique are its high reproducibility, mass production implementation facilities, and low cost. The electroless reduction of platinum salts has been already used, for example, for the deposition on Ti[12] and Si[15] substrates, but to our knowledge, the platinum electroless process has not been reported on a SnO_2 substrate, and Sn(II) has not previously been used as reducing agent for platinum.

In fact, considering the method used in the case of Pd,[14] two main differences arise when trying to extend it to Pt or other metals, resulting from their different chemical properties. First, with respect to the metal salt, $PtCl_2$ cannot be used because it is only soluble in concentrated HCl. Consequently, we use $(NH_4)_2PtCl_4$, which allows for the easy dissolution of Pt(II) and also avoids possible contamination coming from the salt

* To whom correspondence should be addressed. Fax: (+34) 934021231. E-mail: raul@megazero.sct.ub.es.
† Department of Physical Chemistry.
‡ Enginyeria i Materials Electrònics, Department of Electronics.

(1) Brattain, W. H.; Bardeen, J. *Bell Syst. Technol. J.* **1953**, *32*, 1.
(2) Seiyama, T.; Kato, A.; Fujisishi K.; Nagatoni, M. *Anal. Chem.* **1962**, *34*, 1052.
(3) Taguchi, N. Japanese Patent 45-38200, 1962.
(4) Schweizer-Berberich, M.; Zheng, J. G.; Weimar, U.; Göpel, W.; Bârsan, N.; Pentia E.; Tomescu, A. *Sens. Actuators B* **1996**, *31*, 71.
(5) Göpel, W. *Sens. Actuators* **1989**, *16*, 167.
(6) Xu, Ch.; Tamaki, J.; Miura N.; Yamazoe, N. *Sens. Actuators B* **1991**, *3*, 147.
(7) Li, G. J.; Zhang, X. H.; Kawi, S. *Sens. Actuators B* **1999**, *60*, 64.
(8) Yamazoe, N. *Sens. Actuators B* **1991**, *5*, 7.
(9) Gaidi, M.; Chenevier B.; Labeau, M. *Sens. Actuators B* **2000**, *62*, 43.
(10) Sauvan, M.; Pijolat, C. *Sens. Actuators B* **1999**, *58*, 295.
(11) Diéguez, A.; Vilà, A.; Cabot, A.; Romano-Rodríguez, A.; Morante, J. R.; Kappler, J.; Bârsan, N.; Weimar, U.; Göpel, W. *Sens. Actuators B* **2000**, *68*, 94.
(12) Kokkinidis, G.; Papoutsis, A.; Stoychev, D.; Milchev, A. *J. Electroanal. Chem.* **2000**, *486*, 48.
(13) Cabot, A.; Arbiol, J.; Morante, J. R.; Weimar, U.; Bârsan, N.; Göpel, W. *Sens. Actuators B* **2000**, *70*, 87.
(14) Díaz, R.; Arbiol, J.; Cirera, A.; Sanz, F.; Peiró, F.; Cornet, A.; Morante, J. R. *Chem. Mater.* **2001**, *13*, 4362.
(15) Gorostiza, P.; Díaz, R.; Servat, J.; Sanz, F.; Morante, J. R. *J. Electrochem. Soc.* **1997**, *144*, 909.

10.1021/cm011256m CCC: $22.00
Published on Web 06/22/2002

cation because NH_4^+ is easily eliminated by annealing. For platinum, two oxidation states form stable chlorides, i.e., Pt(II) and Pt(IV), and Pt(II) salts are preferred over Pt(IV) salts because the electroless process for obtaining the metal is easier and faster, as previously reported.[16] The second difference with respect to Pd arises from the anion. Thus, if we try to use HCl and $SnCl_2$ with $(NH_4)_2PtCl_4$, a process competitive with electroless deposition occurs. This competitive process, basically due to precipitation process, has not yet been studied in detail, but it is probably due to either the precipitation of $PtCl_2$ or to the formation of some Pt−Sn complex in solution, as has been observed elsewhere[17,18] upon the mixing of tin(II) chloride and platinum(II) chloride. Therefore, sulfate was chosen as the anion both because it prevents this competitive process and because sulfate can also be easily eliminated by annealing.

Thus, SnO_2 nanopowders with platinum coming from a solution containing $(NH_4)_2PtCl_4$ and deposited via a single-step electroless process with $SnSO_4$ acting as the reductor were obtained. The metal salt and reductor concentrations in solution were varied in the solution to analyze their influence on the final catalyst atomic percentage on SnO_2. Different annealing temperatures were also used for the samples to determine their influence on the chemical composition of the sample.

Experimental Details

The preparation of catalyzed tin oxide was achieved by a process similar to that previously described.[14] In the present study, we used an $(NH_4)_2PtCl_4$ aqueous solution with the corresponding platinum concentration, thus adding a freshly prepared aqueous solution of $SnSO_4$ in 2.5×10^{-2} M H_2SO_4. In this case, the addition of the acid facilitates Sn(II) dissolution, and the acid concentration used was chosen to give a pH similar to those used in previous electroless studies.[14]

The basic electroless deposition process is an electronic exchange

$$Pt^{2+} + Sn^{2+} \rightarrow Sn^{4+} + Pt \qquad E° = 0.604\ V$$

which, in practice, can be decomposed into the following half-cell processes linked by conduction through the solid

$$(PtCl_4)^{2-} + 2e^- \rightarrow Pt + 4Cl^- \text{ (metal reduction)} \qquad E° = 0.755\ V^{19} \quad (1a)$$

$$Sn^{2+} \rightarrow Sn^{4+} + 2e^- \text{ (oxidation)} \qquad E° = -0.151\ V^{19} \quad (1b)$$

We used three different nominal atomic Pt/Sn ratios: 0.2, 2, and 10% in atomic concentration. These ratios were tried to study the whole range of the usual concentrations used for gas-sensing applications of Pt addition on SnO_2.[20] For each Pt/Sn ratio, two different concentrations of $SnSO_4$ in the final solution were used: either the stoichiometric Pt^{2+}/Sn^{2+} ratio or 10 times this ratio. Afterward, filtration using model 420 Albet filters was performed, followed by rinsing with diluted H_2SO_4 and then with water. A final desiccation process at 80 °C was performed to collect the final powder.

Then, a thermal treatment was applied to some of the obtained powders using a muffle furnace. This treatment consists of 8 h of heating in air at the desired temperature (either 200, 450, or 800 °C), reached at a rate of 20 K min^{-1}.

X-ray diffraction (XRD) patterns, Raman analysis, X-ray photoelectron spectroscopy (XPS) data, and induced coupled plasma-optical emission spectroscopy (ICP-OES) measurements were collected with the previously described equipment.[14]

For the ICP analysis, the same reported chemical dissolution process[14] was applied. As in the previous case, each dissolution was measured separately by ICP-OES. This chemical process is not able to distinguish between different oxidation states or platinum compounds, and thus, we will refer to total platinum, i.e., the total amount of platinum coming from either metallic platinum, $PtCl_2$, PtO, PtO_2, or any other platinum compound.

Transmission electron microscopy (TEM) was carried out as previously reported.[14] Lattice spacing values obtained from image processing were compared with those published in JCPDS lists for SnO_2[21] and Pt.[22]

All solutions were prepared with p.a.-grade reagents and triply distilled water, which is also used for all water rinses. The chemicals used were $(NH_4)_2PtCl_4$ (99.9%) and SnO_2 (99.9%) (from Alfa), H_2SO_4 (95−97%) from Merck, and $SnSO_4$ (95%) from Aldrich.

Results and Discussion

Figure 1 shows the XRD diffractograms of the sample containing the highest catalyst percentage ratio, which are very similar to the diffractogram obtained for the blank sample (i.e., that of polycrystalline SnO_2[21]), with an additional phase attributed to the added catalyst. The mean grain size of the SnO_2 powder used has been previously reported.[14] For all samples, that not annealed (Figure 1a), that annealed at 450 °C (Figure 1b), and that annealed at 800 °C (Figure 1c), extra peaks corresponding to metallic polycrystalline platinum[22] are observed. Considering the platinum peaks, it can be seen that, for both unannealed samples and samples annealed at low temperature, these peaks are wide, thus indicating that the procedure is good enough to form nanoclusters of metallic platinum at concentrations as high as nominal 10 atom %, greater than the usual concentrations used for gas-sensing applications. Moreover, these nanoclusters still remain at annealing temperatures at least as high as 450 °C, and only annealing at 800 °C makes the metallic platinum XRD peaks narrower, indicating the tendency to form larger clusters at high annealing temperatures, as observed elsewhere.[20] The narrow peaks at an annealing temperature of 800 °C are also observed for intermediate catalyst concentrations (although the relative areas of the peaks with respect to that of tin oxide are smaller). For samples with a nominal 0.2 atom % concentration of catalyst, no evidence of platinum phases is observed because the abundance of these phases lies below the XRD detection limit, but the same behavior would be expected, as will be discussed.

Raman spectra of the whole set of samples show, among all possible SnO_2 Raman bands,[23,24] those bands currently detected, namely, A_{1g} (630 cm^{-1}), B_{2g} (774 cm^{-1}), and E_{1g} (472 cm^{-1})[25] (Figure 2). There are no

(16) Gorostiza, P. Ph.D. Thesis, Universitat de Barcelona, Barcelona, Spain, 1999. Available at http://www.qf.ub.es/a2/nano/index.html.
(17) Cramer, R. D.; Jenner, E. L.; Lindsey, R. V.; Stolberg, U. G. *J. Am. Chem. Soc.* **1963**, *85*, 1691.
(18) Davies, A. G.; Wilkinson, G.; Young, J. F. *J. Am. Chem. Soc.* **1963**, *85*, 1692.
(19) Lide, D. R. *Handbook of Chemistry and Physics*, 78th ed.; CRC Press: Boca Raton, FL, 1997.
(20) Labeau, M.; Gautheron, B.; Cellier, F.; Vallet-Regi, M.; Garcia, E.; González Calbet, J. M. *J. Solid State Chem.* **1993**, *102*, 434.
(21) *JCPDS* **1997**, 41-1445.
(22) *JCPDS* **1997**, 04-0802.
(23) Scott, J. F. *J. Chem. Phys.* **1970**, *53*, 852.
(24) Katiyar, R. S.; Dawson, P.; Hargreave, M. M.; Wilkinson, G. R. *J. Phys. C* **1971**, *4*, 2421.

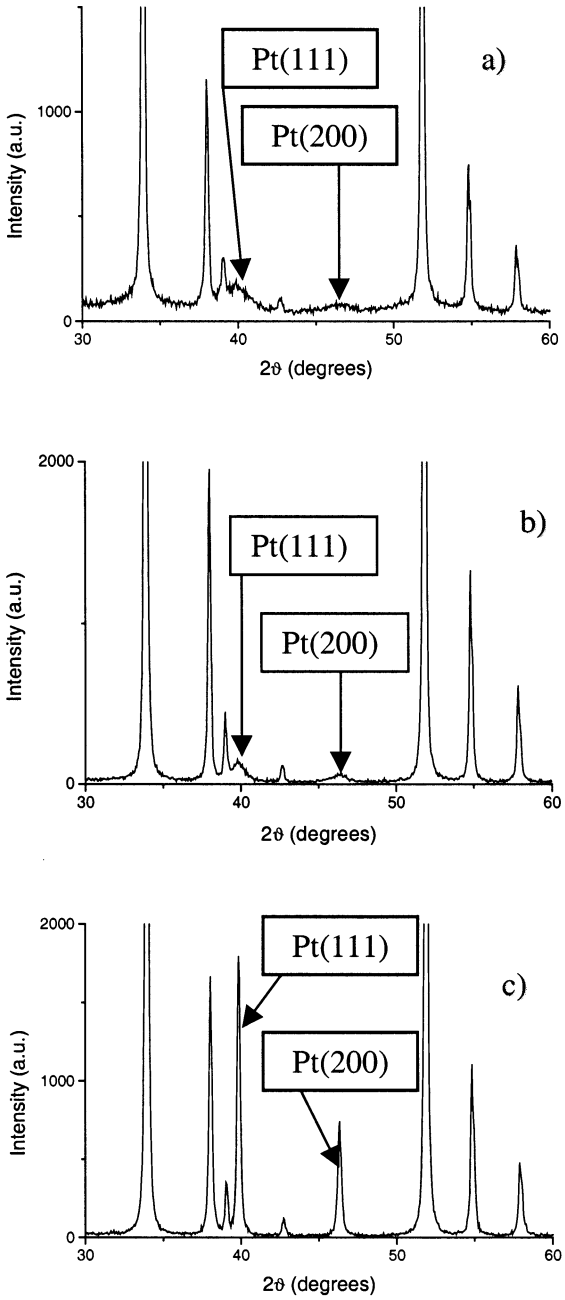

Figure 1. XRD diffractograms of SnO_2 samples obtained from solutions with nominal 10 atom % Pt and a $SnSO_4$ concentration of 10 times the stoichiometric ratio: (a) unannealed, (b) annealed at 450 °C, (c) annealed at 800 °C.

noticeable differences in the spectra for the different annealing temperatures applied (Figure 2a) or for the different catalyst concentrations (Figure 2b). This confirms that the main oxidation state at all annealing temperatures corresponds to metallic platinum, because Raman would not detect metallic platinum because of its high reflectivity to the laser radiation used in these measurements, whereas the presence of any other platinum compound at sufficiently high concentration would have induced additional Raman bands. In addition, although the Raman spectrum of PtO has not previously been reported, all of the results presented in this work are in accordance with this conclusion. This is in

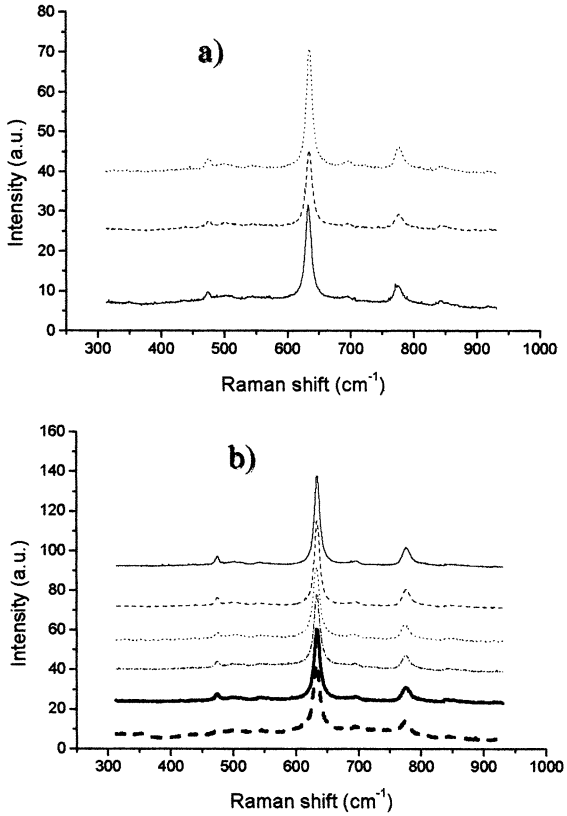

Figure 2. Raman spectra obtained from samples: (a) with nominal 10 atom % Pt and a $SnSO_4$ concentration of 10 times the stoichiometric ratio: —, unannealed; - - -, annealed at 200 °C; • • •, annealed at 800 °C; (b) Samples annealed at 450 °C: —, nominal 0.2 atom % Pt and stoichiometric $SnSO_4$; - - -, nominal 0.2 atom % Pt and a $SnSO_4$ concentration of 10 times the stoichiometric ratio; • • •, nominal 2 atom % Pt and stoichiometric $SnSO_4$; — - — nominal 2 atom % Pt and a $SnSO_4$ concentration of 10 times the stoichiometric ratio; —, nominal 10 atom % Pt and stoichiometric $SnSO_4$; --, nominal 10 atom % Pt and a $SnSO_4$ concentration of 10 times the stoichiometric ratio.

contrast to the results obtained for palladium electroless addition,[14] where the metallic state was predominant at low annealing temperatures whereas PdO was primarily present at high annealing temperatures. Moreover, after annealing, palladium induced a displacement of the Raman bands that we attributed to the incorporation of palladium into the SnO_2 structure. This is not the case for platinum, allowing us to speculate that the incorporation of platinum into the SnO_2 structure is poor. This issue will be discussed again below.

To determine where the catalyst is distributed in the SnO_2 nanopowders, we have also investigated the XPS response of the differently prepared samples. The spectra of the sample with the highest catalyst concentration both unannealed and annealed at 800 °C are shown in parts a and b of Figure 3, respectively. All of the spectra were fitted to reach the right carbon position (284.5 eV).[26] Fittings were performed considering 80/20% Gaussian/Lorentzian orbital peaks and Shirley baselines,[27] and the fitting results verify the presence of metallic platinum ($4f_{7/2}$ peak at 71.2 eV)[28] and also of Pt(II) at all annealing temperatures. Pt(II) is mainly

(25) Yu, K. N.; Xiong, Y.; Liu, Y.; Xiong, C. *Phys. Rev. B* **1997**, *55*, 2666.

(26) Chastain, J. *Handbook of X-ray Photoelectron Spectroscopy*; Perkin-Elmer Corporation: Minneapolis, MN, 1992.
(27) Shirley, D. A. *Phys. Rev. B* **1972**, *5*, 4709.
(28) Cahen, D.; Lester, J. E. *Chem. Phys. Lett.* **1973**, *18*, 108.

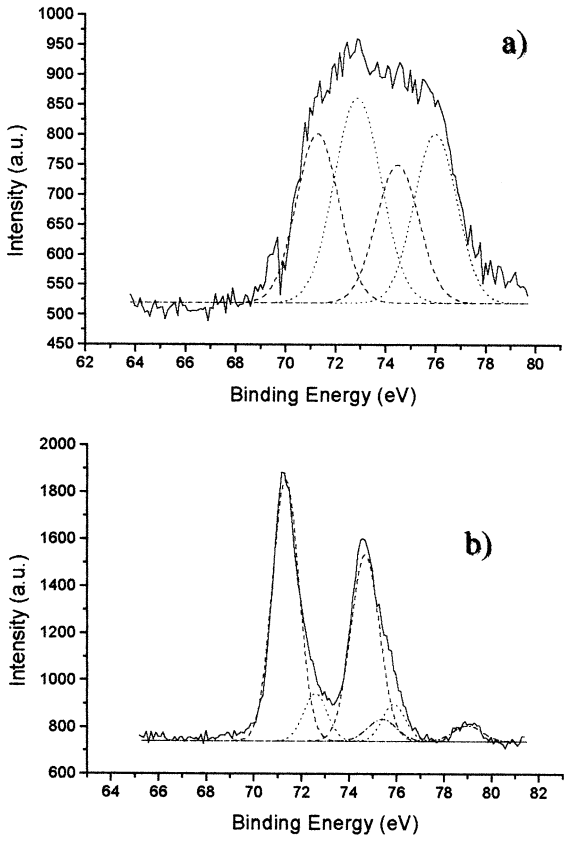

Figure 3. XPS spectra of the samples with nominal 10 atom % Pt and a $SnSO_4$ concentration of 10 times the stoichiometric ratio. (a) Unannealed: —, acquired spectrum; - - -, metallic Pt; • • •, $PtSO_4$. (b) Annealed at 800 °C: —, acquired spectrum; - - -, metallic Pt; • • •, PtO; - • -, PtO_2. The spectra exhibit the 4f doublets of the various Pt species, i.e., for each $4f_{7/2}$ peak, there is its counterpart $4f_{5/2}$ peak shifted toward higher binding energies by about 3−3.5 eV.

present as sulfate at low annealing temperatures and as PtO ($4f_{7/2}$ peak at 72.7 eV)[29] at temperatures of 450 or 800 °C, where we also note the presence of a higher valence state of platinum, Pt(IV), as PtO_2 ($4f_{7/2}$ peak at 75.0 eV)[30] on the surface. With respect to these fitting results, the fact that the areas of platinum(II) sulfate are similar to those of metallic platinum might be because XPS is a surface analytical technique, thus indicating that there is a greater amount of sulfate in the surface than in the bulk. Nevertheless, metallic platinum is the primary species at all annealing temperatures, because it is the only phase detected by XRD and HRTEM, and no platinum bands are detected in Raman. Moreover, the PtO present after annealing in air might probably come from the initial $PtSO_4$, whereas PtO_2 might probably come from the disproportion reaction of Pt(II). XPS results also show that sulfur was completely eliminated only after annealing at 800 °C.

TEM analysis of the sample with highest catalyst concentration annealed at 450 °C shows a homogeneous distribution of the Pt nanoclusters on SnO_2 nanoparticles (Figure 4a). We calculated the mean nanocluster size from TEM micrographs and obtained a mean nanocluster diameter of 4.2 ± 0.8 nm (Figure 4b). These nanoclusters were also analyzed by means of HRTEM and identified as metallic Pt, in accord with the XPS and XRD results, thus confirming that Pt nucleates on the SnO_2 surface as metallic nanoclusters.

The sample with the highest catalyst concentration annealed at 800 °C (Figure 4c) also showed metallic Pt nanoclusters, although these clusters are not homogeneously distributed on the SnO_2 nanoparticle surface and, moreover, they appear in much lower quantity than for annealing at 450 °C. These Pt nanoclusters range in size between 2 and 5 nm. Figure 4c shows an example of a Pt nanocluster on the SnO_2 grain surface. Notice that, in this case, the (200) (interplanar distance = 0.196 nm) platinum planes are parallel to the (110) (0.335 nm) SnO_2 plane.[21,22] The epitaxial growth structure of metal clusters formed on the oxide surface has been studied and communicated elsewhere.[31−33]

Referring to the tin oxide valence band shape and the electronic states that configure it, there is an extensive bibliography describing the main features not only of the undoped tin oxide[34,35] but also of the platinum-induced surface states.[36] The valence band of samples with different catalyst concentrations annealed at 800 and 450 °C are shown in parts a and b of Figure 5, respectively. Surface states are located between the valence band and the Fermi level, behavior that coincides with data reported previously[13,37] and that must be associated with the influence of the catalyst. The density of surface states increases, of course, with catalyst concentration. Nevertheless, it must be stated that the shape of the valence band of our samples is clearly different from the data reported previously for Pt added by impregnation.[13,37] Thus, when dealing with electroless deposition, the density of population of surface states at 800 °C is similar throughout the entire range of binding energies from the top of the valence band to the Fermi level, indicating that our samples have a more metal-like behavior, which is in agreement with the XRD, Raman, and TEM data presented above. The shapes of the valence bands reported here are also different from those reported for palladium obtained either by impregnation[13,37] or by electroless deposition.[14] Nevertheless, it must be stated that, although the electroless addition of Pt gives valence bands with more metal-like behavior, this does not mean that there is no structural interaction between Pt and SnO_2. Thus, it is clear, from a comparison of the valence bands shown in Figure 5a with that reported for pure metallic Pt,[38] that additional surface states are present in our case.

(29) Kerrec, O.; Devilliers, D.; Groult, H.; Marcus, P. *Mater. Sci. Eng. B* **1998**, *55*, 134.
(30) See: http://www.ukesca.org/data/table.html.
(31) Arbiol, J.; Díaz, R.; Cirera, A.; Peiró, F.; Cornet, A.; Morante, J. R.; Sanz, F.; Mira, C.; Delgado, J. J.; Blanco, G.; Calvino, J. J. *Inst. Phys. Conf. Ser.* **2001**, *169*, 73.
(32) Arbiol, J.; Cirera, A.; Peiró, F.; Cornet, A.; Morante, J. R.; Delgado, J. J.; Calvino, J. J. *Appl. Phys. Lett.* **2002**, *80* (2), 329.
(33) Arbiol, J. Ph.D. Thesis, Universitat de Barcelona, Barcelona, Spain, 2001. Available at http://nun97.el.ub.es/~arbiol/index_ang.html.
(34) Kövér, L.; Moretti, G.; Kovács, Zs.; Sanjinés, R.; Cserny, I.; Margaritondo, G.; Pálinkás, J.; Adachi, H. *J. Vac. Sci. Technol. A* **1995**, *13*, 1382.
(35) Kövér, L.; Kovács, Zs.; Sanjinés, R.; Moretti, G.; Cserny, I.; Margaritondo, G.; Pálinkás, J.; Adachi, H. *Surf. Interface Anal.* **1995**, *23*, 461.
(36) Henshaw, G. S.; Ridley, R.; Williams, D. E. *J. Chem. Soc., Faraday Trans.* **1996**, *92*, 3411.
(37) Diéguez, A. Ph.D. Thesis, Universitat de Barcelona, Barcelona, Spain, 1999. Available at http://nun97.el.ub.es/~dieguez/tesis/initesis.html.
(38) Wilson, K.; Prake, J.; Lee, A. F.; Lambert, R. M. *Surf. Sci.* **1997**, *387*, 257.

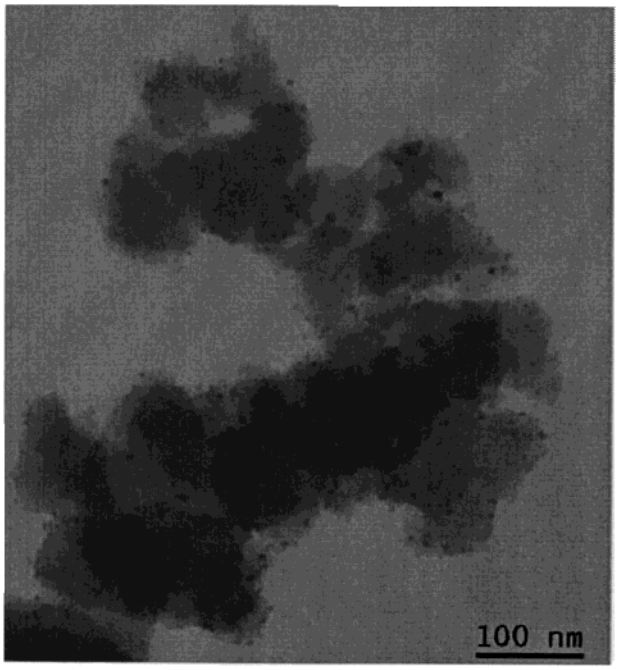

a)

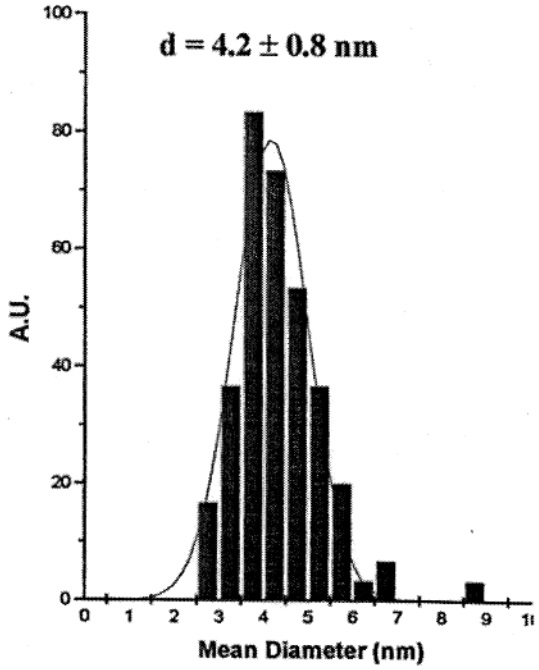

b)

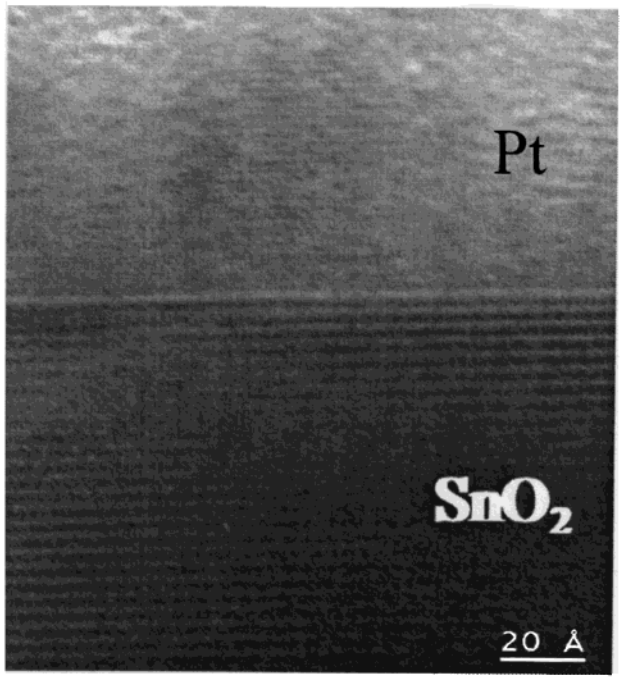

c)

Figure 4. (a) TEM micrograph of the sample with nominal 10 atom % Pt and a $SnSO_4$ concentration of 10 times the stoichiometric ratio annealed at 450 °C. Pt nanoclusters appear in dark contrast on SnO_2 nanopowders. (b) Histogram of Pt nanocluster size for the sample shown in 4a. (c) HRTEM micrograph of a metallic Pt nanocluster present on the sample with nominal 10 atom % Pt and a $SnSO_4$ concentration of 10 times the stoichiometric ratio annealed at 800 °C.

The fact that the valence band of the sample with the highest catalyst percentage that was annealed at 450 °C (Figure 5b) shows a high density of surface states around 3 eV is probably due to the greater amount of Sn(II) compounds coming from the reductor excess present in this sample. This is supported by the facts that the valence band of SnO has been reported to have a maximum density around 3 eV[34] and that the other samples annealed at the same temperature (Figure 5b) all have a much lower density of surface states (even the one with the same nominal Pt concentration but with a stoichiometric concentration of reductor). Moreover, HRTEM analysis of the sample with the highest catalyst concentration annealed at 450 °C also reveals the presence of SnO.

The same shape of surface states is also observed for our samples at lower annealing temperatures, i.e., the valence band shape is similar to that of the sample with

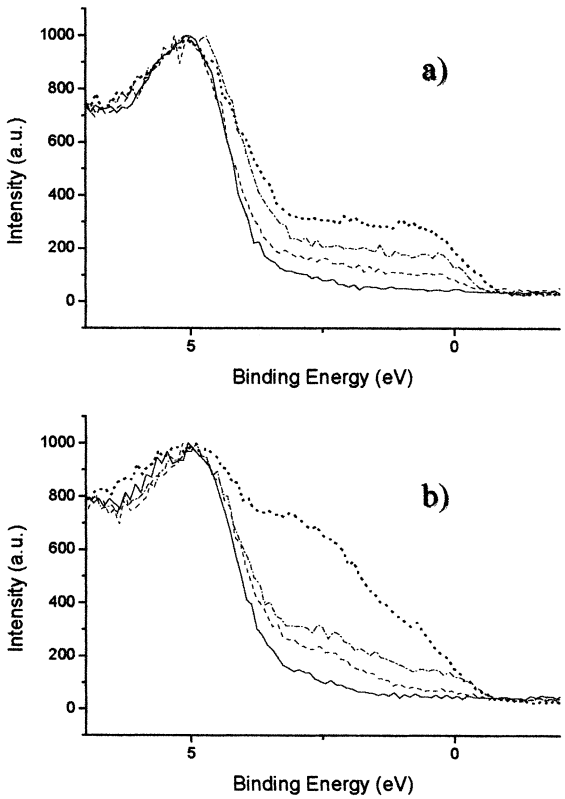

Figure 5. VB spectra for (a) samples annealed at 800 °C with a $SnSO_4$ concentration of 10 times the stoichiometric ratio and (—) nominal 0.2 atom % Pt, (- - -) nominal 2 atom % Pt, (• • •) nominal 10 atom % Pt and samples annealed at 800 °C with a stoichiometric $SnSO_4$ concentration and (- • -) nominal 10 atom % Pt and (b) samples annealed at 450 °C with a $SnSO_4$ concentration of 10 times the stoichiometric ratio and (—) nominal 0.2 atom % Pt, (- - -) nominal 2 atom % Pt, (• • •) nominal 10 atom % Pt and samples annealed at 450 °C with a stoichiometric $SnSO_4$ concentration and (- • -) nominal 10 atom % Pt.

the highest catalyst percentage annealed at 450 °C (Figure 5b) when an excess reductor concentration is present. In contrast, in samples with stoichiometric reductor concentrations, the valence band shape at all annealing temperatures is similar to that observed at 800 °C, thus confirming that the density of surface states associated with platinum is similar throughout the entire range of energies between the Fermi level and the SnO_2 valence band and that the differences in the density of the surface states of different energies arise mainly because of the presence of Sn(II) species.

When comparing the samples annealed at 450 and 800 °C, a greater interaction between Pt and SnO_2 is expected at 450 °C because, as has previously been discussed, at this temperature, there is a greater amount of metallic Pt nanoclusters on the SnO_2 surface. Nevertheless, the HRTEM images shown in Figure 4c also confirm that, even after annealing at 800 °C (where the mean cluster size of Pt increases), there are still some nanoclusters of Pt present on the SnO_2 surface. Moreover, preliminary gas sensor tests of these samples have shown that, for samples annealed at 450 or 800 °C, the gas sensor response with respect to pure tin oxide is improved, thus confirming that an interaction between the added Pt and the SnO_2 surface exists at all annealing temperatures.

Table 1. ICP Results of the Samples with the Highest Catalyst Percentage

nominal Pt/Sn (atom %)	nominal $SnSO_4$/$(NH_4)_2PtCl_4$	anneal temp (°C)	Pt found[a]/ nom Pt (%)	$SnSO_4$ (atom %)	Pt inserted[a]/ total Pt (%)
10	1	–	36.6	0.039	0
10	1	800	25.42	0.0004	3.61
10	10	–	90.5	0.139	0
10	10	800	60.65	0.0008	8.46

[a] Whereas Pt found corresponds to the total amount of Pt present in the samples, the quantity in the last column, labeled Pt inserted, corresponds to only the amount of Pt detected after the third chemical dissolution step.

Other differences are observed when comparing electroless deposition with impregnation. Some of them are discussed below or will be published elsewhere.[39] The differences with respect to the ICP results are summarized in Table 1. They show that the electroless method for catalyst addition to SnO_2 nanopowders is highly efficient, especially when a higher reductor concentration is used. In this case, we find almost 90% of the expected Pt atomic concentration, although the amount of species aggregated from the reductor salt solution is also high. Thus, the efficiency, as obtained from our own results with impregnation under similar conditions (to our knowledge, no ICP results have been reported for Pt added samples), has a value similar to that of classical impregnation and much higher than that obtained by impregnation without evaporation to dryness.[39] In the annealing process, the relative amount of platinum decreases both because some catalyst is lost and also because the reductor species is converted to tin oxide, because almost no reductor species are present after annealing. With respect to the results obtained for Pd electroless deposition,[14] the efficiencies are similar in both cases. A greater effect of the reductor concentration is observed only in the case of platinum, as the efficiencies for the series with a greater reductor concentration are higher than for Pd but those with a stoichiometric reductor concentration are lower. The ICP results showed that, in annealed samples, some platinum still dissolves after the third chemical step. One explanation might be the formation during annealing of species insoluble in aqua regia (as could be the case for some Sn−Pt alloys, as reported elsewhere[40,41]) or the presence of platinum inside the SnO_2 nanopowders, as has also been observed in the case of Pd.[14] Compared to electroless-added palladium,[14] the percentage of platinum dissolved after the third chemical step is much lower, thus confirming the discussion of the coincidence of these results with the Raman shifts observed. Nevertheless, additional studies are needed to determine the origin of this platinum, which represents a maximum of only 8% of the added platinum.

Conclusions

The electroless reduction of $(NH_4)_2PtCl_4$ using $SnSO_4$ as the reductor is reported to produce Pt-added nanoscaled SnO_2 powders. Characterization of these powders shows the feasibility of the proposed catalyst addition

(39) Unpublished results.
(40) Pick, S. *Surf. Sci.* **1999**, *436*, 220.
(41) Rodríguez, J. A.; Jirsak, T.; Chaturvedi, S.; Hrbek, J. *J. Am. Chem. Soc.* **1998**, *120*, 11149.

mechanism as a useful tool for improving existing catalytic materials for use as gas sensors. Promising results have been obtained not only for platinum but also for palladium, currently the two most frequently used additives in gas sensing, even taking into account the differences between the two metals, in terms not only of chemical differences (which can be overcome by changing chemical reagents) but also of the different interactions established with the substrate, as Pd tends to insert into SnO_2 crystallites when annealing in air whereas Pt tends to form large metallic clusters in the same conditions. Moreover, the different chemical state of the catalyst added by electroless deposition compared to that added by classical addition techniques provide us with a new tool for studying the influence of this additive chemical state in the gas-sensing mechanism.

Acknowledgment. The authors thank Tomás Muriel, Josep Lluis Alay, Tariq Jawhari, and Elionor Pèlfort from the XRD, XPS, Raman, and ICP units of the Serveis Científico Tècnics and Ismael Jiménez of the Electronics Department of UB for their cooperation.

CM011256M